

## Titanium Dioxide–Surfactant Mesophases and Ti-TMS1

R. L. Putnam,<sup>†,‡</sup> N. Nakagawa,<sup>†,‡</sup>  
K. M. McGrath,<sup>§,‡</sup> N. Yao,<sup>‡</sup> I. A. Aksay,<sup>†,‡</sup>  
S. M. Gruner,<sup>§,‡</sup> and A. Navrotsky<sup>\*,†,‡</sup>

Departments of Geosciences, Chemical Engineering,  
and Physics, and Princeton Materials Institute  
Princeton University  
Princeton, New Jersey 08544-5263

Received June 12, 1997

Revised Manuscript Received September 4, 1997

Several attempted syntheses of Ti-TMS1, a hexagonal mesoporous TiO<sub>2</sub> reported by Antonelli and Ying,<sup>1</sup> have resulted in a lamellar structure as determined by two-dimensional powder X-ray diffraction and transmission electron microscopy (TEM). Conventional one-dimensional powder X-ray diffraction patterns of the lamellar materials are similar to those reported for Ti-TMS1.<sup>1</sup> Regions, of similar size as those reported to be hexagonal by Antonelli and Ying,<sup>1</sup> of our partially calcined lamellar materials when observed by TEM can be mistaken for hexagonal material. In no cases have we produced specimens that were unambiguously hexagonal. It is concluded that the hexagonal material exists, if at all, only as a minor component of a larger lamellar structure when phosphate surfactants are used, hexagonal Ti-TMS1 therefore remains elusive.

For many years it has been known that some organic compounds, especially surfactants, self-assemble into micellar phases when mixed with water.<sup>2</sup> These micellar phases include lamellar, hexagonal, and cubic structures. In 1992, researchers at Mobil discovered a new family of SiO<sub>2</sub>-based molecular sieves (M41S),<sup>3</sup> formed in a coassembly process<sup>4–7</sup> with a surfactant, which contain hierarchical structures based on the micellar phases formed by the surfactant.<sup>8–10</sup>

Since the Mobil discovery, a new hexagonal mesoporous TiO<sub>2</sub> analogue of M41S called Ti-TMS1, also formed by coassembly with a surfactant, has been

reported by Antonelli and Ying.<sup>1</sup> Additional, related, materials are continuing to be announced<sup>11–15</sup> including a hexagonally packed mesoporous semiconductor, CdS.<sup>16</sup>

The energetics of the M41S and related SiO<sub>2</sub> materials have been studied recently.<sup>17–21</sup> A similar study of Ti-TMS1 materials and other TiO<sub>2</sub> polymorphs would provide data useful for models and generalizations describing the coassembly process and the role of the organic/inorganic interactions. Thus, we have attempted to synthesize the Ti-TMS1 hexagonal phase following the procedure reported by Antonelli and Ying.<sup>1</sup> We discuss here our findings that the hexagonal form has not been reproduced but that the lamellar form is synthesized under a wide variety of conditions.

Antonelli and Ying<sup>1</sup> used tetradecyl phosphate (a 14-carbon chain) as the surfactant in forming their hexagonal mesoporous TiO<sub>2</sub> material. This surfactant was synthesized using well-known reactions.<sup>22</sup> Our work has shown that using commercially available dodecyl phosphate (Alfa/Aesar, a 12-carbon chain) as a surfactant produces conventional powder X-ray diffraction patterns very similar to those published by Antonelli and Ying<sup>1</sup> with the principal peak shifted slightly to higher diffraction angle ( $2\theta$ ) due to the decreased chain length of the surfactant (Figure 1). Such a substitution would have a similar but benign effect in the MCM41 system reported by Beck et al.<sup>3</sup>

All samples were examined using a Scintag PADV powder X-ray diffractometer with  $2\theta/\theta$  geometry. A Cu anode (30 mA and –40 kV) with only K $\alpha$  radiation was used in the diffraction pattern determinations. Further, two-dimensional powder X-ray diffraction of selected samples were obtained using a Rigaku RU-200 rotating anode X-ray diffractometer equipped with a microfocus cup. The generated Cu K $\alpha$  X-rays were focused via bent mirror optics. Images were collected with the Princeton intensifier/lens/ccd area detector.<sup>23</sup> The digital powder diffraction images were azimuthally integrated along an arc of  $\pm 15^\circ$  from the meridional axis to generate one-dimensional plots of scattered intensity versus  $Q = 4\pi \sin \theta/1.54 \text{ \AA}$ , where  $2\theta$  is the angle between the incident and scattered beam directions reproducing those obtained using the Scintag diffractometer. TEM of se-

\* Author for communication: Department of Chemical Engineering and Materials Science, University of California at Davis, Davis, CA 95616. (530) 752-3292.

<sup>†</sup> Department of Geosciences.

<sup>‡</sup> Department of Chemical Engineering.

<sup>§</sup> Department of Physics.

<sup>‡</sup> Princeton Materials Institute.

(1) Antonelli, D. M.; Ying, J. Y. *Angew. Chem., Int. Ed. Engl.* **1995**, *34*, 214.

(2) Tanford, C. *The Hydrophobic Effect: Formation of Micelles and Biological Membranes*; John Wiley & Sons: New York, 1980.

(3) Beck, J. S.; Vartuli, J. C.; Roth, W. J.; Leonowicz, M. E.; Kresge, C. T.; Schmitt, K. D.; Chu, C. T.-W.; Olson, D. H.; Sheppard, E. W.; McCullen, S. B.; Higgins, J. B.; Schlenker, J. L. *J. Am. Chem. Soc.* **1992**, *114*, 10834.

(4) Firouzi, A.; Kumar, D.; Bull, L. M.; Besier, T.; Sieger, P.; Huo, Q.; Walker, S. A.; Zasadzinski, J. A.; Glinka, J. A.; Nicol, J.; Margolese, D.; Stucky, G. D.; Chmelka, B. F. *Science* **1995**, *267*, 1138.

(5) Tanev, P. T.; Pinnavaia, T. J. *Science* **1995**, *267*, 865.

(6) Cheng, C.-F.; He, H.; Zhou, W.; Klinowski, J. *Chem. Phys. Lett.* **1995**, *244*, 117.

(7) Monnier, A.; Schüth, F.; Huo, Q.; Kumar, D.; Margolese, D.; Maxwell, R. S.; Stucky, G. D.; Krishnamurty, M.; Petroff, P.; Firouzi, A.; Janicke, M.; Chmelka, B. F. *Science* **1993**, *261*, 1299.

(8) Cheng, C.-F.; Luan, Z.; Klinowski, J. *Langmuir* **1995**, *11*, 2815.

(9) Fyfe, C. A.; Fu, G. *J. Am. Chem. Soc.* **1995**, *117*, 9709.

(10) Vartuli, J. C.; Schmitt, K. D.; Kresge, C. T.; Roth, W. J.; Leonowicz, M. E.; McCullen, S. B.; Hellring, S. D.; Beck, J. S.; Schlenker, J. L.; Olson, D. H.; Sheppard, E. W. *Chem. Mater.* **1994**, *6*, 2317.

(11) Antonelli, D. M.; Ying, J. Y. *Angew. Chem., Int. Ed. Engl.* **1996**, *35*, 426.

(12) Antonelli, D. M.; Ying, J. Y. *Chem. Mater.* **1996**, *8*, 874.

(13) Luca, V.; MacLachlan, D. J.; Hook, J. M. Withers, R. *Chem. Mater.* **1995**, *7*, 2220.

(14) Zhao, D.; Goldfarb, D. *J. Chem. Soc., Chem. Commun.* **1995**, 875.

(15) Ciesla, U.; Demuth, D.; Leon, R.; Petroff, P.; Stucky, G. D.; Unger, K.; Schüth, F. *J. Chem. Soc., Chem. Commun.* **1994**, 1387.

(16) Braun, P. V.; Osenar, P.; Stupp, S. I. *Nature* **1996**, *380*, 325.

(17) Navrotsky, A.; Petrovic, I.; Hu, Y.; Chen, C.-Y.; Davis, M. E. *Microporous Mater.* **1995**, *4*, 95.

(18) Navrotsky, A.; Petrovic, I.; Hu, Y.; Chen, C.-Y.; Davis, M. E. *J. Non-Cryst. Solids* **1995**, *192*, 474.

(19) Petrovic, I.; Navrotsky, A.; Chen, C.-Y.; Davis, M. E. In *Zeolites and Related Microporous Materials: State of the Art 1994*; Weitkamp, J., Karge, H. G., Pfeifer, H., Hölderich, W., Eds.; *Studies in Surface Science and Catalysis*; Elsevier Science B.V.: Amsterdam, The Netherlands, 1994; Vol. 84.

(20) Petrovic, I.; Navrotsky, A.; Davis, M. E.; Zones, S. I. *Chem. Mater.* **1993**, *5*, 1805.

(21) Kniaz, K.; Navrotsky, A., personal communication. Work still in progress. Princeton University, Department of Geosciences and Princeton Institute.

(22) Cooper, R. S. *J. Am. Oil Chem. Soc.* **1963**, *40*, 642.

(23) Tate, M. W.; Gruner, S. M.; Eikenberry, E. F. *Rev. Sci. Instrum.* **1997**, *68*, 47.

**Table 1. Reactant Ratios for the Synthesis of Mesostructured TiO<sub>2</sub>**

synthesis	pH	Ti:AA:surfactant ratio	mass % surfactant
Antonelli and Ying <sup>1</sup> recommended Ti-TMS1	4–5	1:1:1	7–10
Antonelli and Ying <sup>1</sup> typical synthesis Ti-TMS1 using published molar values	5	1:1:1	9.2
Antonelli and Ying <sup>1</sup> typical synthesis Ti-TMS1 using published mass values	5	2:1:1.4	12.8
this work: lamellar TiO <sub>2</sub> sample from Figure 1a	5	1:1:1	8.37
this work: lamellar TiO <sub>2</sub> sample from Figure 1c	5	1:1:1	7.49

lected samples was performed on a Philips CM20 ST TEM operated at 120 keV.

Fourteen syntheses have been performed using dodecyl phosphate. The first two followed the ratios (1:1:1) for titanium (titanium(IV) isopropoxide, Aldrich), acetyl acetone (Fischer), and surfactant combined in sufficient water to form a solution of 7–10% (by mass) of the surfactant as recommended by Antonelli and Ying.<sup>1</sup> Antonelli and Ying<sup>1</sup> did not explicitly state if the potassium salt of the surfactant (as synthesized) or the protonated form was used. We used both forms. A few syntheses attempted to clarify the inconsistencies between the mass quantities and the molar quantities of reactants in the published typical synthesis for Ti-TMS1 as shown in Table 1. In each case deviation from the recommended 1:1:1 ratio of reactants in a 7–10% (by mass) surfactant solution resulted in poorly crystalline materials.

The difference between the use of the potassium salt or the protonated form of the surfactant is significant since ionic strength is known to affect micellar formation and micelle shape. Also, Antonelli and Ying adjusted the pH with concentrated HCl(aq) and the potassium salt would require more HCl(aq) to obtain the optimal pH range of 4–6. As a result, the concentration of chloride ion would be greater in a preparation using the potassium salt. Chloride ion has been shown to assist in the formation of M41S<sup>24</sup> materials and in the selective formation of crystalline rather than amorphous TiO<sub>2</sub> in the hydrolysis of titanium alkoxides.<sup>25</sup>

Other syntheses were either duplications of those mentioned or modifications showing that similar X-ray diffraction patterns can be obtained using the substitutions listed in Table 2. Two syntheses examined the use of HBr(aq) instead of HCl(aq) since the presence of bromide ion has been shown to select for hexagonal structure over lamellar structure in M41S.<sup>24</sup> No change in the X-ray diffraction pattern was seen.

Figure 1 shows typical powder X-ray diffraction patterns for our samples as well as the pattern for the Ti-TMS1, as reproduced from Figure 5b in the paper published by Antonelli and Ying.<sup>1</sup> Note the similarity between pattern (a) (this work) and pattern (b) (Antonelli and Ying). Because of the similarity in the X-ray diffraction patterns, no attempt at indexing was made until later syntheses when the first hint of a third peak (indexed as 300 in Figure 1) was seen.

Indexing using two-dimensional powder X-ray diffraction patterns confirmed that samples (a) and (c) were lamellar with no measurable hexagonal component. Two-dimensional X-ray diffraction eliminates

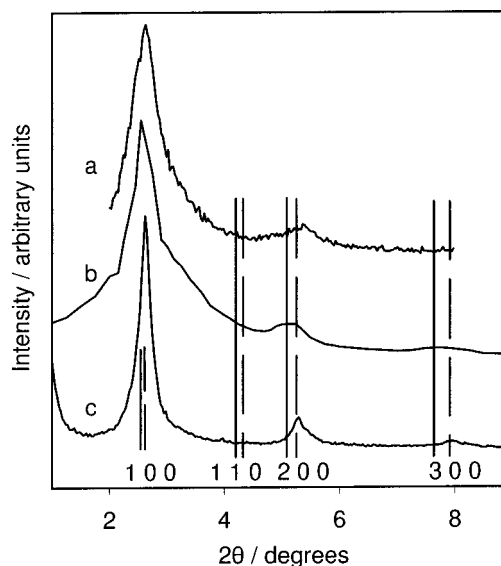


**Figure 1.** Powder X-ray diffraction patterns for (a) lamellar TiO<sub>2</sub>, (b) Ti-TMS1 published as Figure 5b by Antonelli and Ying,<sup>1</sup> and (c) lamellar TiO<sub>2</sub>. Solid vertical lines indicate the calculated locations of the 100, 110, 200, and 300 peaks using a 100 spacing (36 Å) as published by Antonelli and Ying.<sup>1</sup> Dashed lines represent the calculated locations of the 100, 110, 200, and 300 peaks using a 100 spacing (33.5 Å) for syntheses reported in this work. The apparent lateral shift in patterns (a) and (c) with respect to pattern (b) is a result of using a shorter surfactant in the syntheses covered by this work than that used by Antonelli and Ying.<sup>1</sup> Vertical displacement is arbitrary to assist the reader in making comparisons between the three patterns.

**Table 2. Observed Substitutions to the Antonelli and Ying<sup>1</sup> Synthesis Resulting in Similar Powder X-ray Diffraction Patterns**

X	substitutes for
dodecyl phosphate (C <sub>12</sub> OPO(OH) <sub>2</sub> )	tetradecyl phosphate C <sub>14</sub> OPO(OH) <sub>2</sub>
NH <sub>4</sub> OH	KOH
glacial acetic acid	acetyl acetone
dodecylamine	C <sub>14</sub> OPO(OH) <sub>2</sub>
HBr	HCl

effects of possible preferred orientation and has been used extensively in studies of liquid crystals and membranes requiring low-angle X-ray diffraction.<sup>26,27</sup> Pattern (b) in Figure 1 could be better indexed as lamellar, primarily because of the absence of the hexagonal 110 peak that should be found near 4.25° (2θ). (See the solid vertical lines in Figure 1.) Reevaluation of all X-ray data from the syntheses performed in this work confirmed patterns consistent with lamellar structures and prompted examination of these materials with TEM.

Figure 2a shows a TEM image of the sample corresponding to the X-ray diffraction pattern of Figure 1c,

(24) Huo, Q.; Margolese, D. I.; Ciesla, U.; Feng, P.; Gier, T. E.; Sieger, P.; Leon, R.; Petroff, P. M.; Schüth, F.; Stucky, G. D. *Nature* **1994**, *368*, 317.

(25) Henry, M.; Jolivet, J. P.; Livage, J. In *Role of Complexation in the Sol–Gel Chemistry of Metal Oxides, Ultrastructure Processing of Advanced Materials*; Uhlmann, D. R., Ulrich, D. R., Eds.; John Wiley & Sons: New York, 1992; Chapter 3.

(26) Gruner, S. M. *J. Phys. Chem.* **1989**, *93*, 7562.

(27) Hajduk, D. A.; Harper, P. E.; Gruner, S. M.; Honeker, C. C.; Kim, G.; Thomas, E. L.; Fetters, L. J. *Macromolecules* **1994**, *27*, 4063.

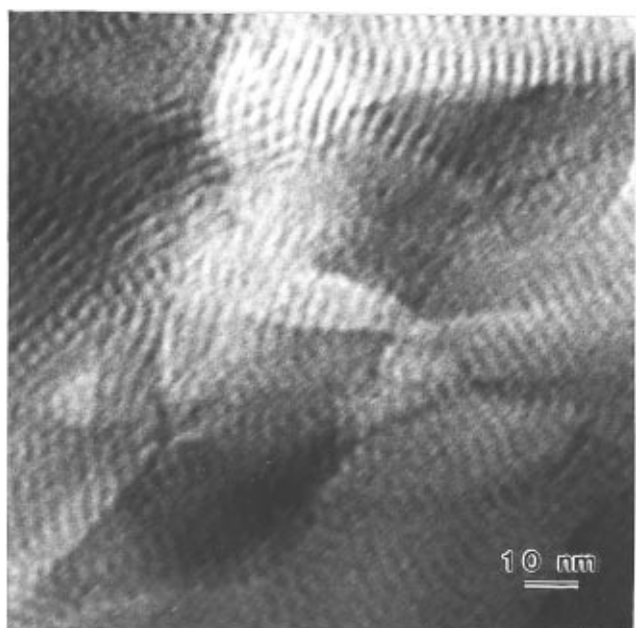
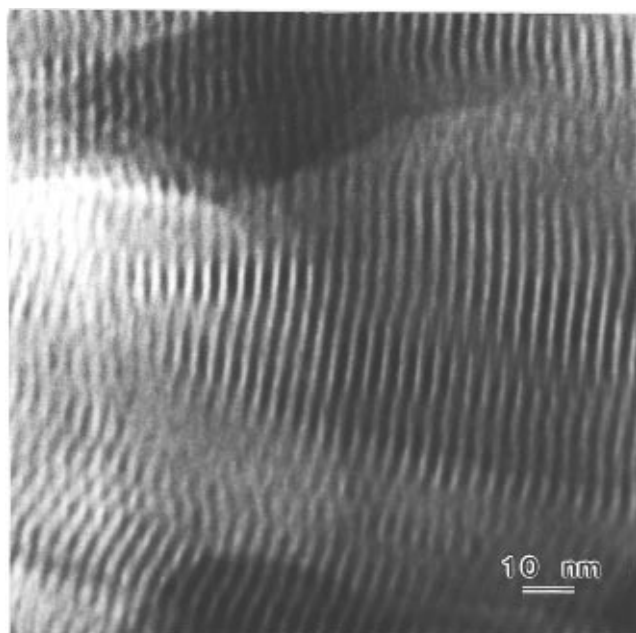


**Figure 2.** (a, top) TEM image of the sample from Figure 1c. The material is lamellar with large domains. (b, bottom) TEM image of the sample from Figure 1a. Note the similar morphology with image (a). This sample is also lamellar with smaller domains.

clearly showing a well-defined lamellar structure with large domains. Similarly, Figure 2b shows a TEM image of the sample corresponding to the X-ray diffraction pattern of Figure 1a, showing a lamellar structure less well defined than that shown in Figure 2a. Both images in Figure 2 are representative of all images obtained for the respective samples.

Attempts at full calcination in air at temperatures as low as 250 °C of the synthesized materials resulted in complete collapse of the structure and a powder X-ray diffraction pattern with no sharp peaks consistent with a totally amorphous structure. Some samples were able to be calcined to approximately 70% surfactant removal (based on thermogravimetric analysis) while retaining some long-range order observable by X-ray diffraction. Nitrogen adsorption on these partially calcined materi-

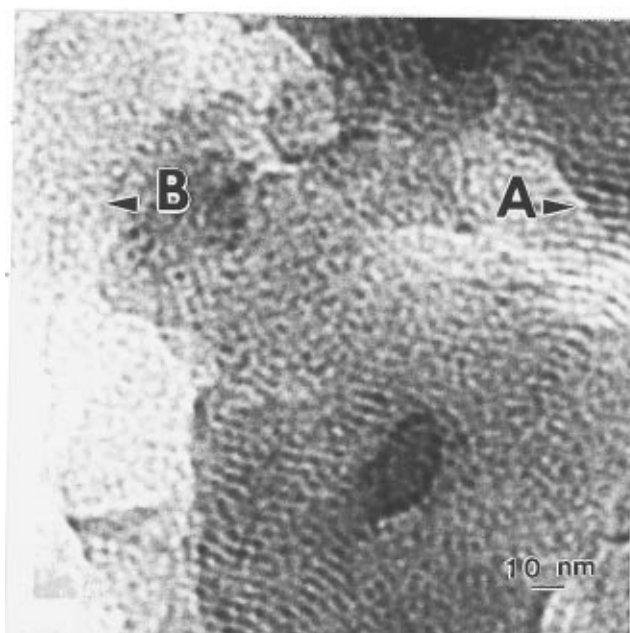


**Figure 3.** Partially calcined material. Note the remnant of lamellar domains indicated in region A. Region B could be mistaken for a not quite ordered hexagonal phase but is in fact a superposition of lamellae.

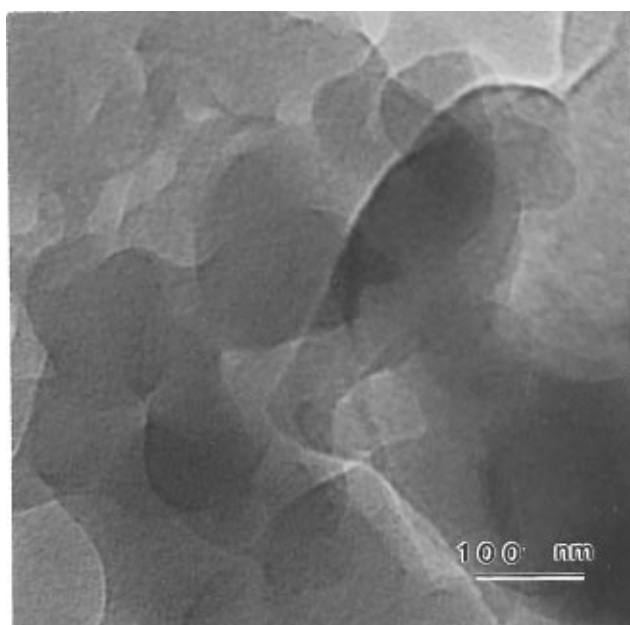


**Figure 4.** Fully calcined material. Note the absence of any previously observed structure. The sample is amorphous and has a plate like layering.

als resulted in BET (BET = Brunauer–Emmett–Teller) surface areas of between 47 and 63 m<sup>2</sup>/g. No material was found with a measurable BET surface area near the 200 m<sup>2</sup>/g reported for Ti-TMS1, indicating that we were unable to reproduce the hexagonal material reported in the original paper.

Partially calcined samples were also viewed using TEM. Figure 3 is representative of all images obtained. Some lamellar regions are still observable in region A but the domain size is greatly reduced. Region B shows noticeable areas that appear to be hexagonal though not well ordered. In every observed field of view these areas appear in regions of thin but overlapping chunks of lamellar material.

Fully calcined samples are amorphous with an overlapping platelike morphology as can be seen in Figure 4. When this amorphous material is calcined further at 500 °C for 24 h, potassium titanium oxyphosphate ( $\text{KTiOPO}_4$ ), potassium titanium phosphate ( $\text{KTi}_2(\text{PO}_4)_3$ ), and anatase ( $\text{TiO}_2$ ) are clearly identifiable in the X-ray diffraction pattern. Partial Rietveld refinement of the diffraction pattern results in the approximate composition 75%  $\text{KTiOPO}_4$ , 14%  $\text{KTi}_2(\text{PO}_4)_3$ , and 14% anatase. Clearly there is significant retention of the phosphate headgroup after calcination.

It is possible that hexagonal  $\text{TiO}_2$  may form through either the published pathway<sup>1</sup> or some other unknown pathway. However, we conclude that it exists, if at all, only as a minor component of a larger lamellar structure when phosphate surfactants are used and therefore remains elusive. Such a coexistence would account for the observations made in our laboratory: calcination results in complete collapse of the structure with retention of the phosphate ion; X-ray diffraction patterns are dominated by lamellar material; transmission electron microscopy images that can be misleading when dealing with lamellar structures.

Lamellar  $\text{TiO}_2$  has been synthesized in a wide variety of conditions. Ti-TMS1 remains difficult to synthesize,

and care must be taken in examining materials thought to be Ti-TMS1, particularly lamellar materials. Partially calcined lamellar structures can be mistaken for the hexagonal material using transmission electron microscopy. The combination of indexing clear X-ray diffraction patterns (preferably two-dimensional powder patterns) with TEM analysis of the resulting materials can help to distinguish the lamellar form of  $\text{TiO}_2$  and its hexagonal relative Ti-TMS1.

**Acknowledgment.** We acknowledge discussions with J. Y. Ying and D. M. Antonelli on the synthesis and characterization of the materials discussed in this paper. P. J. Heaney and D. M. Yates have been helpful through their assistance and instruction on the operation of the Scintag X-ray powder diffractometer at low  $2\theta$  as well as assisting in the Rietveld refinement of the calcined material. Financial support for this research has come from an NSF/MRSEC program (Grant DMR94-00362) and the U.S. Army Research Office (Grant DAAH04-95-1-0102). Instrumentation in S.M.G.'s laboratory is supported through DOE Grant DE-FG02-87ER60522.

CM970419X